Available online at www.sciencedirect.com
SCIENCE DIRECT®
Polymer 44 (2003) 8177–8184
polymer
www.elsevier.com/locate/polymer

Crystalline and viscoelastic properties of branched polyethylenes synthesized using bidentate nickel (II) catalyst

Deuk-Kil Park, Il Kim, Chang-Sik Ha*

Department of Polymer Science and Engineering, Pusan National University, Keumgjung ku, Pusan 609-735, South Korea

Received 7 March 2003; received in revised form 12 August 2003; accepted 8 October 2003

Abstract

In this work, five branched polyethylenes with different branching units were synthesized using bidentate nickel (II) catalyst containing α-diimine ligands. For comparison, one linear polyethylene was also prepared using tridentate iron (II) catalyst containing α-diimine ligand. The crystalline structure of the polyethylenes was investigated using X-ray diffraction (XRD) and polarized optical microscope. The crystalline properties were also measured by differential scanning calorimeter (DSC). Viscoelastic properties of the polyethylenes were investigated using rheometric dynamic analyzer. The DSC and XRD results showed that highly branched polyethylenes exhibit no melting points and no predominating crystalline forms, while the linear polyethylene exhibits clear orthorhombic (110) and (200) reflections on XRD pattern and a clear melting point at 118 °C. The viscoelastic properties of the branched polyethylenes were very complicated due to the combined effect of the molecular weight difference and the degree of chain branching as well as the branching structure.

Keywords: Branched polyethylene; Bidentate nickel (II) catalyst; Chain branching

1. Introduction

One of the main advances in the polyolefin technology in the last decade was the use of single-site metallocene catalysts to produce a new variety of ethylene and α-olefinic copolymers [1]. It enables polyolefinic materials to strengthen their presence in the fields of elastomer and plastomer. The metallocene catalysts permit to improve control of molecular weight (MW), molecular weight distribution (MWD) and short-chain branching (SCB), which can be used to enhance the performance of the final product.

Recently, Du Pont developed the Versipol process, where olefins are polymerized with nickel-diimine complexes as catalyst precursors [2]. These catalysts can make branched ethylene homopolymers in the absence of any α-olefin as a comonomer [3,4]. Short-chain branches are produced through the chain walking mechanism, with no comonomer addition, and the degree of branching can be controlled by reaction parameters such as polymerization temperature, ethylene pressure and type of catalyst precursor and co-catalyst. ^{13}C NMR studies showed that methyl to hexyl branches, or longer, were produced [5,6], although methyl branches were predominant.

The effect of branching in polyethylene has been studied in detail and it is of crucial importance in understanding and predicting polyolefin properties [7]. The presence of chain branches decreases the size of the linear and crystallizable sequences in the backbone, i.e. the size of the lamella thickness [8] thus modifying the morphology and the degree of crystallinity [9]. Also, the added ability to introduce long chain branching (LCB) into what would otherwise be linear polyethylenes has opened up a broad range of processing possibilities. LCB incorporated into the linear copolymers enhances shear thinning and melt elasticity. Yet to be fully determined, however, are the types of long chain branch architectures that most effectively promote these desirable rheological attributes, and to what degree these types are present in metallocene polyolefins [10].

On the other hand, bidentate nickel (II) α-diimine complexes, recently developed by Brookhart et al. [11,12] show a lot of advantages over metallocene catalyst [13]. It makes decreasing the path of synthesis mechanism and decreasing the amount of co-catalyst, methylaluminoxane (MAO). Also one can use another co-catalyst to alternate

* Corresponding author. Tel.: +82-51-510-2407; fax: +82-51-514-4331.
E-mail address: csha@pusan.ac.kr (C.S. Ha).

0032-3861/$ - see front matter © 2003 Elsevier Ltd. All rights reserved.
doi:10.1016/j.polymer.2003.10.021

MAO. Generally, this catalyst is much cheaper than the metallocene catalyst [14]. The properties of polyethylenes prepared with bidentate nickel (II) catalyst, however, were not systematically investigated as yet, although many efforts have been made to correlate molecular structure to mechanical properties in ethylene copolymers [15–17] and in blends of polyolefins [18–20].

In this work, various polyethylenes with different branching unit were synthesized by using bidentate nickel (II) and tridentate iron (II) complexes combined with MAO. The structure of the resulting polyethylenes was characterized by ^{13}C NMR spectroscopy and X-ray diffraction (XRD) measurement. We wish to report how the degree of chain branching and the molecular weight difference of the polyethylenes affect their thermal and viscoelastic properties.

2. Experimental

2.1. Materials

All reactions were performed under a purified argon atmosphere using standard glove box and Schlenk techniques. Polymerization grade of ethylene (SK Corp., Korea) was purified by passing it through columns of Fisher RIDOX catalyst and molecular sieve 5A/13X. MAO was obtained from Akzo Chemical as a 8.4 wt% total Al solution in toluene. Solvents were distilled from Na/benzophenone and stored over molecular sieves (4 Å). Literature procedures were used to synthesize five bidentate nickel (II) complexes [11,12] and a tridentate iron (II) catalyst precusor [21].

2.2. Polymerization

Six different polyethylene samples were synthesized by using five different bidentate nickel (II) catalyst precursors [11,12], and a tridentate iron (II) catalyst precursor [21] in combination with MAO as a cocatalyst. The molecular structure of the catalyst precursors is shown in Fig. 1. Ethylene polymerizations were performed in a 250 mL round-bottom flask equipped with a magnetic stirrer and a thermometer. In a dry box, the reactor was charged with toluene (80 mL) and a prescribed amount of MAO ([Al]/[Ni] = 300). The reactor was immersed in a constant-temperature bath previously set to a desired temperature. When the reactor temperature had equilibrated to the bath temperature, ethylene was introduced into the reactor after removing argon gas under vacuum. When no more absorption of ethylene into toluene was observed, 5 μmol of nickel catalyst dissolved in toluene was injected into the reactor and then the polymerization was started. More detailed information was published elsewhere [22].

2.3. Measurements

The ^{13}C NMR spectra of polymers were recorded at 120 °C on a Varian Unity Plus 300 spectrometer operating at 75.5 MHz. Samples for ^{13}C NMR spectra were prepared by dissolving 50 mg of polymer in 0.5 mL of benzene-d_6/1,2,4-trichlorobenzene-d_3 (1/5 v/v). A total of 6000 transients were accumulated for each spectrum with a 12 s delay between pulses. Decoupling was always on during acquisition so the nuclear Overhauser enhancement was present. The intrinsic viscosity of polymers was determined in decalin at 135 °C using an Ubbelohde viscometer.

XRD measurements were done on a diffractometer by Rigaku Miniflex using nickel-filtered Cu Kα radiation (λ = 0.154 nm) operating at 30 kV and 15 mA. A Thermal analyses TA 100 calorimeter was used to determine melting temperatures. Samples were heated from room temperature to 180 °C, held at this temperature for 5 min, cooled down to −50 °C, and then heated again to 180 °C. The heating and cooling rates were 10 °C/min. The analyses were performed under nitrogen flux. Melting temperatures were determined in the second scan.

A LEICA DMRXP microscope with polarized light equipped with a hot stage was used to study the morphology and crystallization of the polyethylenes. Images were captured using HITACHI KP C550 CCD color camera. The samples between glass slides and cover slips in a hot stage to 180 °C for 5 min prior to rapid cooling to the isothermal crystallization temperature. The isothermal crystallization temperature was selected as 70 °C. After a time long enough for the polyethylene samples to crystallize completely (approximately 1 h), the glass slides were taken out of the hot stage and were quenched in ice water.

Rheological measurements were carried out on a rheometric dynamic analyzer (RDAII). The dynamic viscoelastic properties were determined with frequencies from 0.1 to 100 rad/s. Prior to performing frequency sweeps, strain sweeps were performed to establish the linear region at each frequency. Measurements were carried out in nitrogen atmosphere at 190 °C.

3. Results and discussion

3.1. Structure determination

All catalysts used in this study contain pyridine diimine ligands of general structures shown in Fig. 1. The key to high polymer production using the aryl-substituted α-diimine systems is the incorporation on the aryl rings of bulky *ortho* substituents that greatly retard the rate of chain transfer. It is well-known that the bidentate nickel (II) catalysts give highly branched polyethylene and the tridentate iron (II) catalyst highly linear polyethylene [11,12,21]. In this sense, we utilized various nickel (II) complexes by changing the bulkiness of the ligand and an

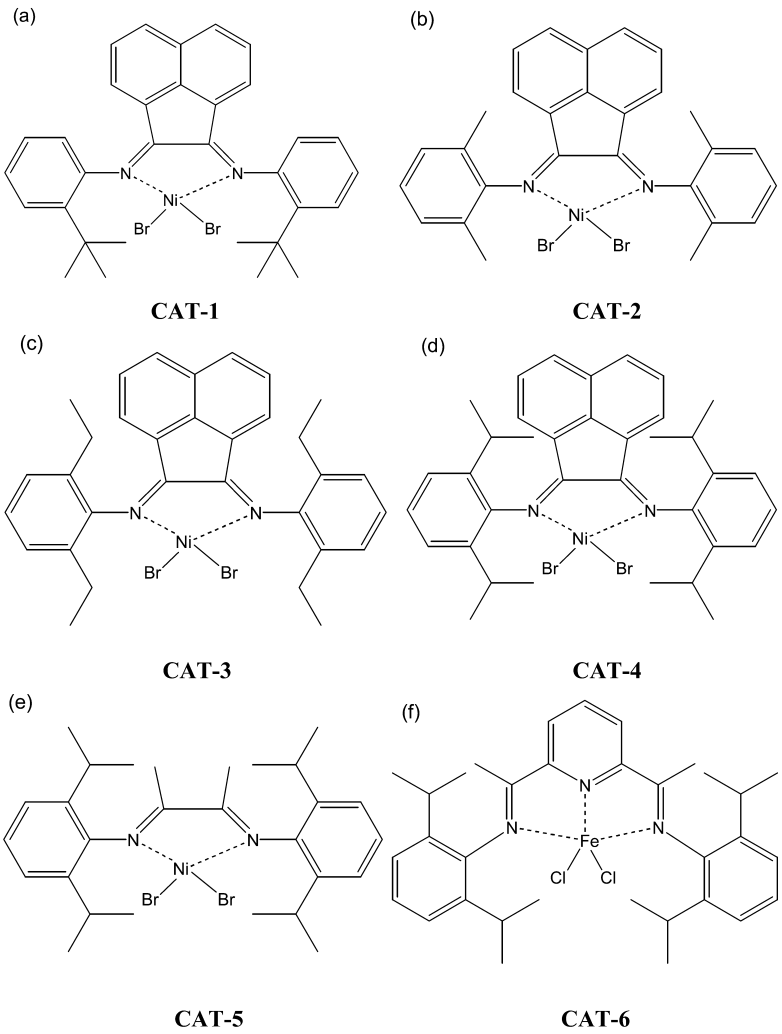

Fig. 1. Bidentate nickel (II) catalysts and a tridentate iron (II) catalyst used in this work.

iron catalyst in order to get polyethylene samples with different degree of branching and molecular weight. Table 1 shows viscosity-average molecular weights (M_v) of the six polyethylenes produced with various catalysts. It was found that the polyethylene by CAT-5 (cat5PE) has the highest M_v (173,500 g/mol) and the polyethylene by CAT-2 (cat2PE) has the lowest M_v (22,470 g/mol), while cat1PE, cat3PE, and cat4PE possess similar molecular weights. These results show that the relative rate of propagation versus chain transfer in the bulky α-diimine system allows for the formation of high molecular weight polymer in contrast to most late metal systems.

Table 1
Viscosity-average molecular weights of polyethylenes synthesized in this work

Sample	M_v
cat1PE	58,100
cat 2PE	22,470
cat 3PE	52,575
cat 4PE	64,900
cat 5PE	173,500
cat 6PE	87,800

The highly linear homopolymer (cat6PE) to highly branched low-density polyethylenes (cat3PE, cat4PE, and cat5PE) could also be prepared by changing the structure of the ligand and by employing different metal. The steric bulk of the catalysts was influenced by systematically varying the backbone and *ortho*-aryl substituents of the α-diimine ligand. Typical ^{13}C NMR spectra of the polyethylenes are shown in Fig. 2 for cat3PE (a) and cat6PE (b). The largest resonance, which occurs at 30.0 ppm, is due to the methylene carbons on the backbones and on the long chain branches (LCB) [23]. The resonances for the α, β, and γ carbons occur at 34.6, 27.2, and 32.2 ppm, respectively. The LCB was quantified by comparing the LCB methine resonance (38.2 ppm) to the methylene resonance. Paired 1,2 and 1,3 methyl branches were not found since resonances close to 16.64 and 40 ppm came from 1,2-$1B_1$ and 1,3-$\alpha'B_1$ carbons, respectively. Paired 1,4 methyl branches were identified by the presence of the resonances at 19.99 ppm of 1,4-$1B_1$ carbon, the resonances at 33.543,

33.476, and 33.409 ppm corresponding to the 1,4-brB_1 carbon, and the resonances at 34.785 and 34.731 ppm corresponding to the 1,4-$\alpha'B_1$ carbon. The resonances of 1,4-brB_1 and 1,4-$\alpha'B_1$ are split due to the presence of meso and racemic structures [23]. Paired 1,5 methyl branches were identified by the resonance of the 1,5-$\beta'B_1$ carbon at 24.61 ppm. The presence of 1,6 paired methyl branches was confirmed by the resonance of the 1,6-$\beta'B_1$ carbon at 27.79 ppm, and the other resonances are superimposed. The absence of 1,7 paired methyl branches is suggested by the absence of 1,7-$\beta'B_1$ resonances assigned by Cheng [24] at 30.8 ppm. Methyl branches with spacing longer than seven carbons appear as isolated branches.

The presence of short chain branches as ethyl, butyl, and amyl was identified by the resonances of specific carbons. Due to the low content of these branches, the existence of short paired branches seems improbable, and in fact, these branches were not found. The most surprising feature in this work was the presence of a good number of long branches ($n \geq 6$). These branches are confirmed by the presence of 3Bn and 4Bn at 32.16 and 29.59 ppm, respectively. Due to the high content of these branches it seems reasonable to identify the 1,4 paired branches by the resonances at 31.50 and 38.24 ppm assigned to the carbon 1,4-α'Bn and 1,4 brBn (Fig. 2).

Other samples were also analyzed by the same method as for cat3PE and cat6PE and the result are summarized in Table 2. On increasing the steric size of the backbone and *ortho*-aryl substituents of the α-diimine ligand in Ni (II) complexes, higher molecular weight and more highly branched ethylene homopolymers result. Sterically encumbered diimine ligands prevent associative exchange following the formation olefin-hydride species [11,12]. The olefin-hydride species can reinsert olefin with opposite regiochemistry generating new active species which introduce short chain and/or LCB into the growing polymer chains.

Table 2
Branch distribution in polyethylenes catalyzed by bidentate nickel (II) [(a) cat1PE through cat5PE] and tridentate iron (II) complexes [(b) cat6PE], which is analyzed by ^{13}C NMR spectroscopy

Branch	Sample (percentage of branching, mol%)					
	cat 1PE	cat 2PE	cat 3PE	cat 4PE	cat 5PE	cat 6PE[a]
Methyl(total)	6.29	3.94	3.23	0.61	4.75	–
Methyl-1,4	2.33	1.53	3.50	7.61	7.71	–
Methyl-1,5	0	0	1.50	3.00	1.12	–
Methyl-1,6	2.41	1.47	3.76	4.77	6.77	–
Ethyl	0.30	1.23	2.81	4.01	2.54	–
Propyl	0	1.66	1.38	1.02	0.37	–
Butyl	0.08	0.96	2.42	6.23	2.96	–
Amyl	0.16	0.32	0.60	1.02	0.75	–
Long	1.04	1.81	2.16	0.09	2.10	–
Long-1,4	0.12	0.22	0.88	1.80	0.56	–
Total	12.73	13.14	22.24	30.16	29.63	0

[a] The linear polyethylene cat 6PE was prepared with a tridentate iron (II) catalyst for comparison.

Accordingly, chain transfer is believed to be an important factor to decide the degree of chain branching. In contrast to the Ni (II)-diimine catalysts, no branching is observed for the cat6PE using a tridentate iron (II) catalyst, even with the bulky ligand containing isopropyl group in the 2,6-position of the aryl ring.

3.2. Crystalline structure

Fig. 3 shows differential scanning calorimeter (DSC) melting traces of the bidentate nickel (II) catalyzed polyethylenes as well as the linear cat6PE. The cat6PE had the crystallization peak temperature at 118 °C. The polyethylenes with long chain branching did not exhibit any crystalline melting peaks of high density polyethylene. The melting points were decreased with increasing chain branching. In this way, there are no melting points for cat3PE, cat4PE, and cat5PE. Since the branch content of cat6PE was not measured by ^{13}C NMR (Table 2), its higher T_c and higher T_m suggest that cat6PE has fewer branches than the others. DSC thermograms for the samples with high branching (cat1PE–cat5PE) failed to give useful information about branch distribution.

The crystalline structure of the bidentate nickel (II) catalyzed polyethylenes with different branching was measured using XRD. The XRD patterns of the polyethylenes are shown in Fig. 4 (cat1PE–cat5PE (a) and cat6PE (b)). One main strong diffraction peak with a weak shoulder was observed, respectively, at 21.5 and 23.8° for both cat1PE and cat2PE samples with relatively SCB due to the orthorhombic (110) and (200) reflections, but only a broad amorphous halo was observed around 19° for other highly branched polyethylenes, cat3PE, cat4PE and cat5PE samples. The amorphous character of those highly branched polyethylenes (cat3PE, cat4PE and cat5PE) is in accordance with the DSC results in Fig. 3. The cat6PE, however, showed clearly the orthorhombic (110) and (200) reflections along with some weaker reflections from other planes. The XRD analysis was followed by McFaddin et al. and Butler et al. [25,26].

Fig. 5(a) and (b) show typical polarized optical micrographs of cat2PE and cat6PE, respectively. It is clearly shown that cat6PE exhibits traces of polyethylene spherulites, whereas cat2PE with long chain branching does not exhibit any traces of polyethylene spherulites due to its nearly amorphous nature.

3.3. Viscoelastic properties

On the other hand, the systematic study of the relationships between the molecular structure and the rheological behavior of polyolefins has been seriously limited in the past by the lack of samples with controlled and simply described distributions of molecular weight and LCB [27]. Polymers prepared using traditional catalyst systems have a fairly broad MWD that is difficult to

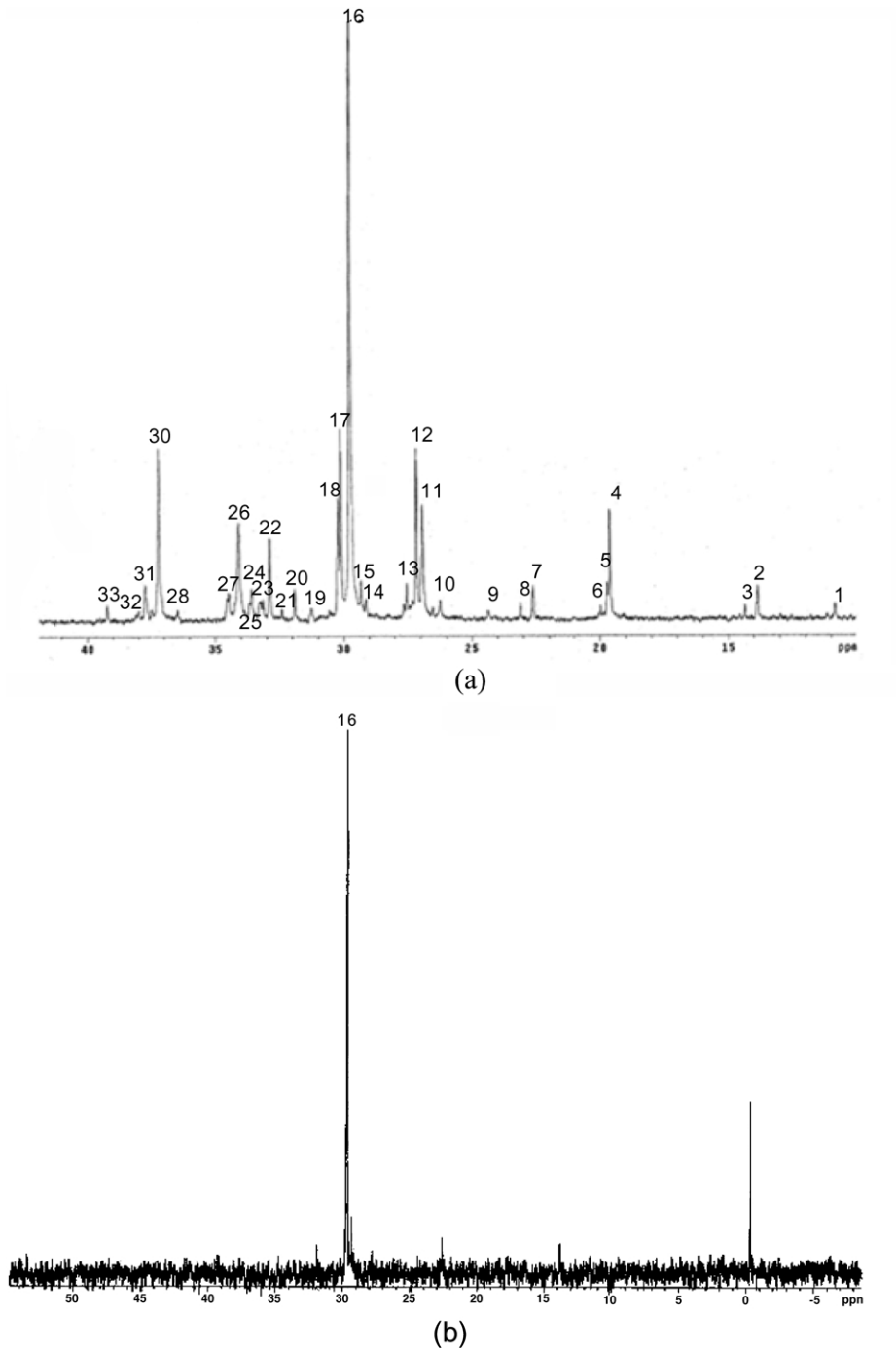

Fig. 2. Typical ^{13}C NMR spectra of polyethylenes synthesized by CAT3 [cat3PE] (a) and CAT6 [cat6PE] (b).

reproduce. While the preparation of monodisperse samples continues to be problematic, single site catalysts now make it possible to prepare samples in which the MWD is relatively narrow and quite reproducible [28].

The degree, length, and structure of the branching all affect the rheological behavior in various ways. Recently, Wood-Adams et al. [27] reported the effects of weight average molecular weight (M_w) and short and long chain branching on the linear viscoelastic behavior of polyethylene (and ethylene-α-olefin copolymers). Yan et al. [29] studied the effect of LCB on rheological properties of the metallocene polyethylene. In the work, they produced a series of branched polyethylenes having approximately the same M_w and narrow MWD using their high temperature and high pressure continuous stirred tank reactor and Dow Chemical GCG-Ti catalyst system. The LCB densities were in the range of 0–0.44 branch per 10,000 carbons. The polyethylene samples were systematically investigated in terms of their rheological and mechanical properties. The LCB resulted in steady-state viscosity increase and melt

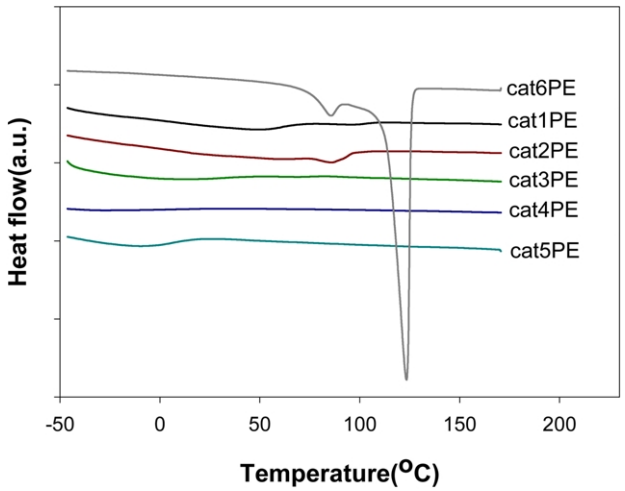

Fig. 3. DSC thermograms of polyethylenes catalyzed by bidentate nickel (II) complexes (cat1PE through cat5PE) and tridentate iron (II) complexes (cat6PE).

flow reduction. The enhancement of shear-thinning properties was particularly spectacular in the view of such low LCB density levels.

It must be noted at this point that since the impact of

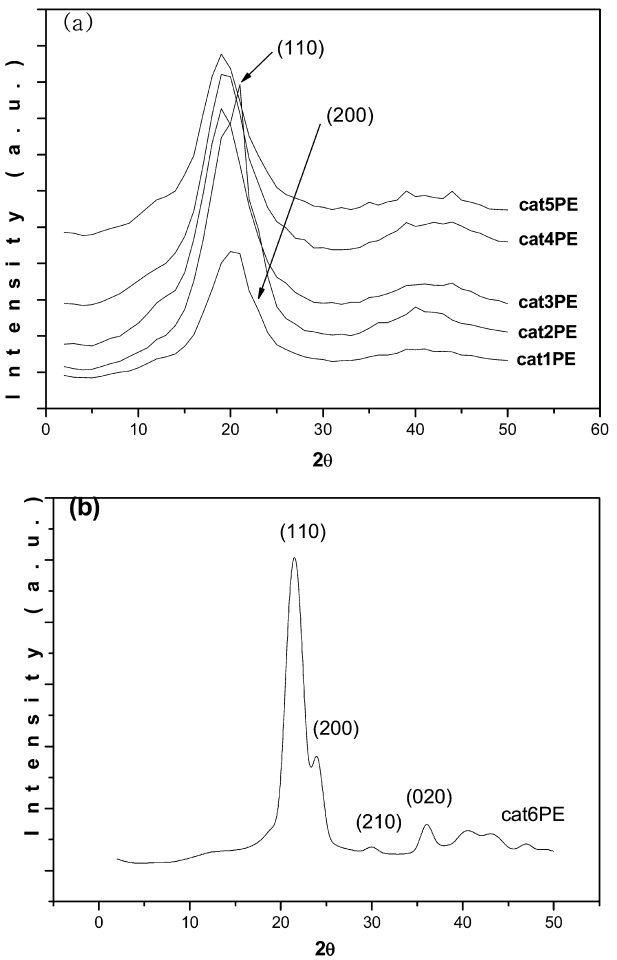

Fig. 4. XRD patterns of polyethylenes catalyzed by bidentate nickel (II) [(a) cat1PE through cat5PE] and tridentate iron (II) complexes [(b) cat6PE].

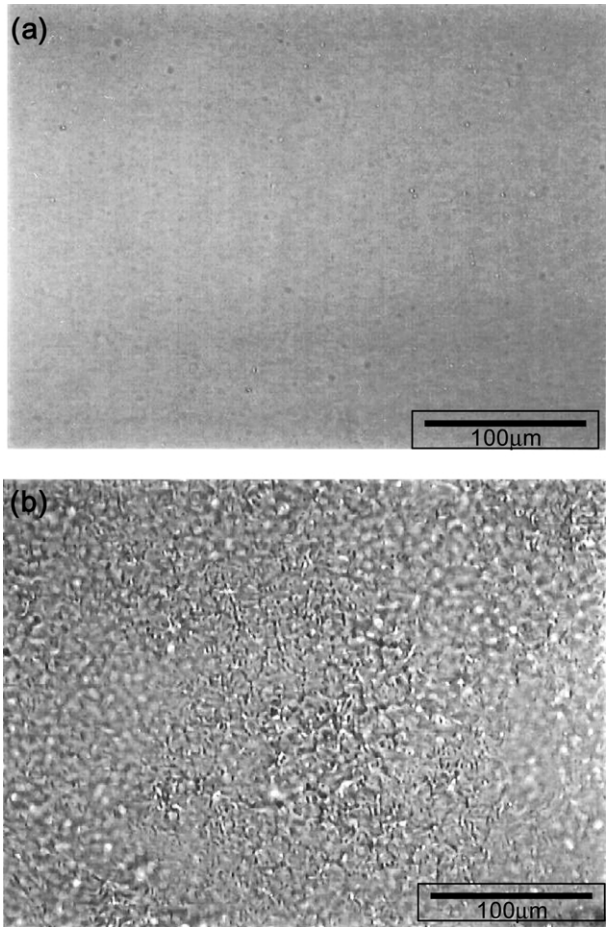

Fig. 5. Polarized optical micrographs of (a) cat2PE and (b) cat6PE.

LCB on the rheological behavior is determined not only by the number of branch points but also by the branch length distribution and architecture. Generally, LCB affects the complex viscosity in four ways [25]: (1) the zero shear viscosity is increased for the same backbone molecular weight, (2) the amount of shear thinning is increased, (3) the transition zone between the zero shear viscosity and the power law zone is broadened and (4) two points of injection appear within the transition zone.

Fig. 6 gives the complex viscosity data at different shear rates (0.1–100 rad s^{-1}) for six polyethylene samples with different branch distributions at 190 °C. The cat6PE with no branching showed higher complex viscosities than those of other branched polyethylenes except cat5PE, while cat2PE showed the lowest complex viscosities. A comparison of Fig. 5 and Table 1 clearly indicates that the differences in the complex viscosities are primarily due to the molecular weight difference. An increase in molecular weight causes an increase in the zero shear viscosity and a decrease in the frequency at which shear thinning begins. It is generally known that the branched polyethylene gives higher viscosities than their linear counterparts. In Fig. 6, however, it is seen that the complex viscosities of the polyethylenes in

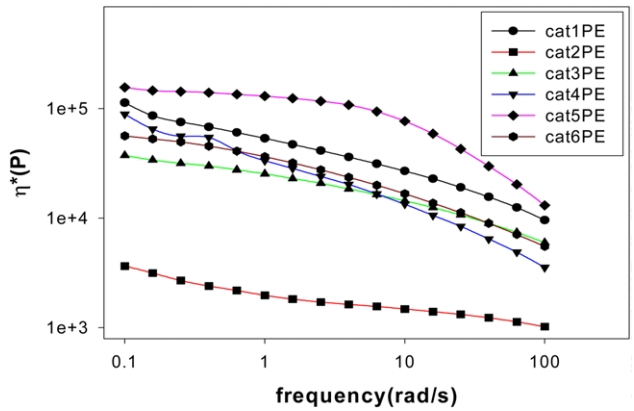

Fig. 6. Complex viscosity of polyethylenes catalyzed by bidentate nickel (II) [cat1PE through cat5PE] and tridentate iron (II) complexes [cat6PE] at 190 °C.

the shear frequency ranges were not significantly affected by the degree of branching.

The storage moduli are shown in Fig. 7. The main reason for the diversity in Fig. 7 is their molecular weight difference as for the complex viscosities. The higher M_v samples exhibited the higher storage modulus. In this way, cat5PE which has the highest M_v value (173,500 g/mol) shows the highest storage modulus.

The ratio of loss modulus and storage modulus (tan δ) is given in Fig. 8. The tan δ behavior as a function of frequency is very complex due to the combined effect of chain branching and molecular weight difference. A general observation is that cat3PE has the highest tan δ and cat4PE shows the lowest tan δ values over the whole frequency region except cat5PE and cat2PE, which show abnormal tan δ behaviors compared to others. The tan δ values showed maxima at a certain frequency for the cat2PE and cat5PE, though the frequency at which tan δ showed a maximum was different. Tables 1 and 2 show that the molecular weight deceased in the order cat5PE $\gg$ cat6PE $>$ cat1PE $\approx$ cat3PE $\approx$ cat4PE $>$ cat2PE and the degree of branching is decreased in the order cat4PE $\approx$

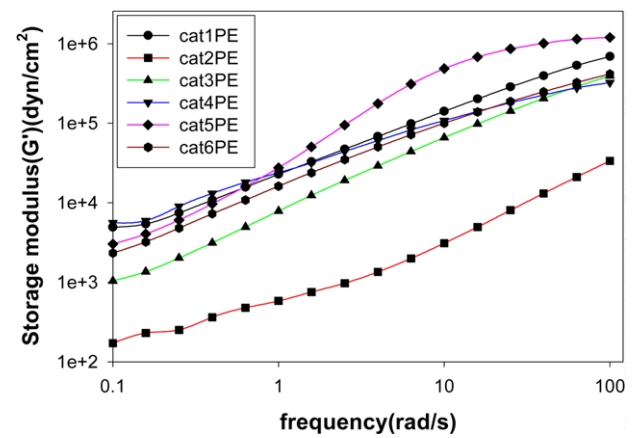

Fig. 7. Storage modulus versus shear rate at 0.1–100 rad/s for polyethylenes catalyzed by bidentate nickel (II) [cat1PE through cat5PE] and tridentate iron (II) complex [cat6PE].

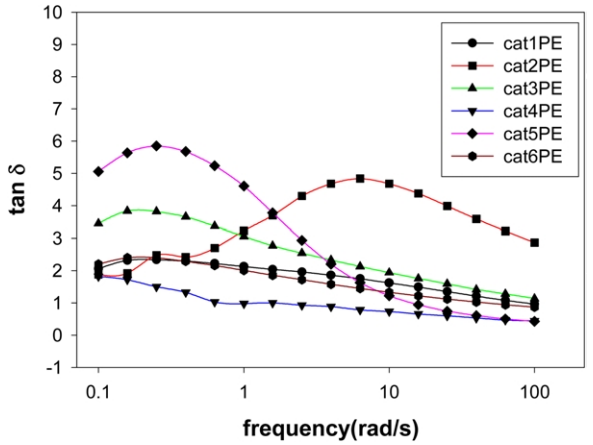

Fig. 8. Tan $\delta(G''/G')$ versus shear rate at 190 °C for polyethylenes catalyzed by bidentate nickel (II) [cat1PE through cat5PE] and tridentate iron (II) complexes [cat6PE].

cat5PE $>$ cat3PE $>$ cat2PE $\approx$ cat1PE $>$ cat6PE. If one compare the tan δ behaviors of cat3PE and cat4PE, the absolute tan δ values are related to the different degree of chain branching since their molecular weights are similar. Harrel and Nakajima [30] reported that the G' and G'' vs. frequency plot can be used for analyzing the effect of chain branching. The low frequency branching and, thus, for the extreme case, the G' response dominates over the entire range of observed frequencies: that is, no $G'-G''$ crossover (tan $\delta = 1$) is observed. Therefore, the lowest tan δ values close to the unity for cat4PE is mainly due to the long chain branching, which usually shows viscous properties. Other polyethylenes show elastic properties over the whole frequency region since the tan δ is larger than the unity [31].

Comparison of the tan δ behaviors of cat1PE and cat2PE, however, indicates that the tan δ behaviors are related to their molecular weight difference, since their degree of chain branching is almost same. The occurrence of maxima in tan δ at low frequency for cat5PE may be also due to its high molecular weight. The difference in the frequency at which the tan δ shows maxima is clearly due to the effect of different molecular weight when one consider the difference in their molecular weights. Such speculation is evident if one compare the tan δ behaviors as a function of frequency of cat6PE with no branching and those of cat4PE with highest degree of branching are similar each other except the absolute tan δ values.

Another reason of such complex tan δ behaviors may be also due to different structure of chain branching. Table 2 shows, for instance, cat4PE has largest amounts of butyl group in the branch but cat5PE has largest amounts of methyl group in the branch among the six polyethylenes, although the total degree of branching is almost same.

4. Conclusions

In this work, six different branched polyethylenes were

obtained with bulky α-diimine catalysts of nickel (II) and iron (II). The bidentate nickel (II) catalyst combined with MAO gave branched polyethylenes, while the tridentate iron (II) catalyst linear polyethylene. The DSC and XRD results showed that highly branched polyethylenes (cat3PE, cat4PE and cat5PE) exhibit no melting points and no predominating crystalline forms, while the linear cat6PE polyethylene exhibits clear orthorhombic (110) and (200) reflections, characterized by the peaks at 21.5 and 23.8°, on XRD pattern and a clear melting point at 118 °C. One main strong diffraction peak with a weak shoulder was observed, respectively, at 21.5 and 23.8° for both cat1PE and cat2PE samples with relatively SCB due to the orthorhombic (110) and (200) reflections, but only a broad amorphous halo was observed around 19° for other highly branched polyethylenes, cat3PE, cat4PE and cat5PE samples.

The viscoelastic properties of polyethylene samples were very complicated due to the combined effect of molecular weight difference and the degree of chain branching as well as the branching structure. The differences in the complex viscosity curves are primarily due to molecular weight variation. An increase in molecular weight causes an increase in the complex viscosity. Similar results were also found for the storage moduli behaviors.

The tan δ behavior as a function of frequency was very complex due to the combined effect of chain branching and molecular weight difference as well as the different chain branching structure. A general observation is that cat3PE has the highest tan δ and cat4PE shows the lowest tan δ values over the whole frequency region except cat5PE and cat2PE, which show abnormal tan δ behaviors compared to others. The tan δ values showed maxima at a certain frequency for the cat2PE and cat5PE, though the frequency at which tan δ shows a maximum is different.

Acknowledgements

This work is supported by the National Research Laboratory Program, the Center for Integrated Molecular Systems, POSTECH, Korea, Brain Korea 21 Project, and the Center for Ultramicrochemical Process System. The authors thank Prof. Y.K. Han of Hanyang University, Korea for his help in the microscopic measurements.

References

[1] Montagna AA, Burkhart RM, Dekmezian AH. Chemtech 1997;12:26.
[2] Johnson LK, Killian CM, Brookhart MS. US Patent 96/23010, 1996.
[3] Rol W, Brintzinger HH, Rieger B, Zolk R. Angew Chem Int Ed Engl 1990;29:279.
[4] Brookhart M, Johnson LK, Killian CM, Mecking S, Tempel DJ. ACS Polym Prep 1996;37(2):254.
[5] Simon LC, Oaares JBP, deSouza RF. AIChE J 2000;46:1234.
[6] Jurkiewicz AA, Eilerts NW, Hsieh ET. Macromolecules 1999;32: 5471.
[7] Mandelkern L. J Phys Chem 1971;75:3909.
[8] Flory PJ. J Am Chem Soc 1962;84:2857.
[9] Glotin M, Mndelkern L. Macromolecules 1981;14:1394.
[10] Bubeck RA. Mater Sci Eng R 2002;39:1.
[11] Brookhart M, Jhonson LK, Killian CM, Arthur SD, Feldman J, McCord EF, McLain SJ, Kreutzer KA, Bennett AM, Coughlin BE, Ittel SD, Parthasarathy A, Tempel DJ. USA Patent Application WO 96/23210, 1996.
[12] Johnson LK, Killian CM, Brookhart M. J Am Chem Soc 1995;117: 6414.
[13] Scharrer E, Brookhart M. J Organomet Chem 1995;497:61.
[14] Kim I, Kim SM, Ha YS, Han BH. Polym Sci Technol 2001;12:331.
[15] Simanke AG, Galland GB, Freitas L, da Jornada JAH, Quihada R, Mauler RS. Polymer 1999;40:5489.
[16] Brooks NW, Duckett RA, Ward IM. Polymer 1999;40:7367.
[17] Simake AG, Galland GB, Baumhardt N, Neto R, Quijada R, Mauler RS. J Appl Polym Sci 1999;74:1194.
[18] Loos J, Bonnet M, Petermann JJ. Polymer 2000;41:351.
[19] Madar D, Thomann Y, Suhm J, Mulhaupt R. J Appl Polym Sci 1999; 74:838.
[20] Rana D, Chon K, Woo T, Lee B, Choe S. J Appl Polym Sci 1999;74: 1169.
[21] Small BL, Brookhart M. J Am Chem Soc 1998;120:7143.
[22] Simon LC, de Souza RF, Mauler RS. J Polym Sci, Part A: Polym Chem 1999;37:4656.
[23] Galland GB, de Souza RF, Mauler RS, Nunes FF. Macromolecules 1999;32:1620.
[24] Cheng HN. Polym Bull 1986;16:445.
[25] McFaddin DC, Russell KE, Kelusky EC. Polym Commum 1986;27: 204.
[26] Butler MF, Donald AM, Bras W, Mant GR, Derbyshire GE, Ryan AJ. Macromolecules 1995;28(19):6383.
[27] Wood-Adams PM, Dealy JM, deGroot AW, Redwine AD. Macromolecules 2000;33:7489.
[28] Raju VR, Smith GG, Marin G, Knox JR, Graessley W. J Polym Sci, Polym Phys Ed 1979;17:1183.
[29] Yan D, Wang WJ, Zhu S. Polymer 1999;40:1737.
[30] Harrel ER, Nakajima N. J Appl Polym Sci 1984;29:995.
[31] Kim Y, Ha CS, Kang T, Cho WJ. J Appl Polym Sci 1994;51:1453.